

# CHARACTERIZING RATE INHIBITION IN H<sub>2</sub>O/H<sub>2</sub> GASIFICATION VIA MEASUREMENT OF ADSORBED HYDROGEN CONCENTRATION

M. G. Lussier, Z. Zhang, and D. J. Miller

Department of Chemical Engineering  
Michigan State University  
East Lansing, MI 48824

Keywords: Gasification, Kinetics, Rate Inhibition

## INTRODUCTION

Gasification of coal for fuels production is not currently used on a wide scale because extreme conditions are needed to achieve reasonably fast reaction rates. One reason for these extreme conditions is the inhibition of gasification by hydrogen in the reacting gas phase. For example, gasification rate decreases by an order of magnitude with the addition of only 1 ppm hydrogen to steam [1], and rate has been shown to decline significantly with conversion in hydrogen and steam/hydrogen mixtures [2,3]. Hydrogen dissociatively chemisorbed onto carbon is very stable, generally accepted as dissociative in nature, and requires temperatures approaching 1800 K to completely desorb [4].

The three possible modes of hydrogen inhibition in steam gasification are as follows [3]:



Selection of any of the possible inhibition modes gives the following basic rate expression [3,5]:

$$\text{rate}_{co} = \frac{C_A K_1 P_w}{1 + K_2 P_w + K_3 P_H^n} \quad (4)$$

Dissociative adsorption gives a value of 0.5 for  $n$  [3], which has been found to be the case for low hydrogen pressures [6] and subatmospheric steam pressures [7]. Reverse oxygen exchange and associative hydrogen adsorption both give values of one for  $n$ , as reported in earlier studies [5,8,9]. Associative adsorption has been found to contribute to inhibition at higher pressures, but dissociatively bound hydrogen still dominates char surfaces [10].

## EXPERIMENTAL

A char of Dow Saran Resin (MA 127) was prepared in a quartz tube reactor at 1173 K in flowing nitrogen for 0.5 hr., ground and sieved to -60+100 mesh, then annealed in an alumina reactor at 5 K/min to 1773 K in flowing argon for 6 hr.

Chars were gasified inside a quartz lined Inconel 625 differential packed bed microreactor which was housed inside a larger pressure vessel capable of simultaneous operation at 1273 K and 6.6 MPa. The entire system was designed to have absolute minimal internal volume to facilitate accurate measurement of transient species. After gasification in 40% steam and various proportions of argon and hydrogen at 1123 K and pressures ranging from 0.3 to 3.3 MPa, rapid switching to pure argon was done and transients monitored. The inherent system transient response was accounted for by using 1% krypton as a tracer in the reactant gas argon.

After gasification, chars were removed, weighed, and placed inside the alumina reactor for temperature programmed desorption (TPD) to measure the quantity of adsorbed hydrogen. Samples were outgassed in argon at 10 K/min to 1773 K in a Mellen split tube furnace with a programmable temperature controller. Effluent species from both reactors were analyzed with an Ametek M100M Quadrupole Mass Spectrometer, which is interfaced with a personal computer for data collection and deconvolution.

## RESULTS

Figures 1 and 2 show rate curves for steam/hydrogen gasification of annealed Saran char at 1.0 MPa and 3.1 MPa total pressure, 1123 K, 40% steam, and varying concentrations

of hydrogen balanced with argon. The CO + CO<sub>2</sub> formation rate is independent of steam partial pressure at these conditions when no hydrogen is present in the reactant gas, and hydrogen inhibition of CO + CO<sub>2</sub> formation is clearly observable with increasing hydrogen partial pressure. Methane formation rate is approximately first order in hydrogen partial pressure and independent of steam partial pressure. A decline in rate is also observed over the first 1% conversion when hydrogen is present in the reactant gas for both CO + CO<sub>2</sub> formation and methane formation; this decline becomes more pronounced under higher hydrogen partial pressures. In the most extreme case, CO + CO<sub>2</sub> formation rate approaches zero at 1.0 MPa total pressure and 0.6 MPa hydrogen partial pressure. All rate curves gradually increase with conversion after the first 1%, which follows the increase in char surface area. Figure 3 shows char surface areas as determined by N<sub>2</sub> BET analysis, indicating a very highly porous material is formed with conversion.

Figure 4 shows adsorbed hydrogen on a per unit weight basis as a function of char conversion following gasification. Surprisingly, adsorbed hydrogen concentration is only a function of conversion and not reactant gas composition. There appears to be two zones of adsorption behavior. The first is an initial rapid adsorption to almost 30 ccH<sub>2</sub>(STP)/g up to 1% conversion, and the second is a more gradual but steady increase in adsorbed hydrogen to 100 ccH<sub>2</sub>/g at 70% conversion. The hydrogen peak maximum is at 1500 K during TPD, indicating that hydrogen is dissociatively adsorbed on the char surface.

Figure 5 shows adsorbed hydrogen concentration following gasification on a per unit area basis. The increase in adsorbed hydrogen with conversion after the initial rapid adsorption stage is partially accounted for by the increase in char surface area with conversion; however, the gradual increase in adsorbed hydrogen concentration per unit area indicates that hydrogen continues to adsorb onto the char throughout the entire course of gasification.

Figure 6 shows CO + CO<sub>2</sub> formation rate during a reaction in which hydrogen fraction of the reactant gas is cycled between 0% and 60%. A rate curve from a steam only gasification has been included for reference. Rate reversibly changes from a value close to that of the reference curve to a very low value as hydrogen is added and excluded from the reactant gas. This indicates that steady state rate is only a function of reactant gas composition.

## DISCUSSION

Our results support both reverse oxygen exchange and dissociative hydrogen adsorption as modes of inhibition in steam/hydrogen gasification of chars, with reverse oxygen exchange acting throughout the course of reaction and dissociative hydrogen adsorption inhibiting rate only upon initial exposure to hydrogen. Temperature programmed desorption studies show that dissociative hydrogen adsorption occurs throughout gasification, most rapidly during the first 1% conversion. There may be a relationship between this initial rapid adsorption and the rate decline over the same initial 1% conversion for chars exposed to hydrogen-containing reactant gases; however, the same initial rapid hydrogen adsorption is not accompanied by a decline in rate when there is no hydrogen present in the reactant gas. Conversion beyond the first 1% is also marked by an increase in adsorbed hydrogen, albeit much less rapidly, but not by a decline in rate. Step changes in reactant gas compositions result in gasification rates that reach steady-states which are similar to those achieved with unchanging reactant gas compositions.

This leads to the conclusion that, at high conversions (>1%) the adsorbing hydrogen does not compete for the same active sites at which gasification occurs. If the dissociative hydrogen adsorption measured by TPD has blocked sites active in gasification, the increase in surface hydrogen concentration would lead to a corresponding decrease in the total number of active sites and thus a decrease in gasification rate regardless of reactant gas composition. This does not occur.

At low conversion, however, dissociative hydrogen adsorption may play a role. At high hydrogen partial pressures, reverse oxygen exchange cannot be solely responsible for hydrogen inhibition because it is driven by hydrogen partial pressure which is not changing during the initial rapid decline in rate. It appears that dissociative hydrogen adsorption contributes to rate inhibition by competing with oxygen exchange for active sites. Upon initial exposure of the char to a reactant gas with a high hydrogen partial pressure, a greater proportion of active sites become blocked with dissociatively adsorbed hydrogen over the course of 1% conversion. Once the rapid transient adsorption is complete, an

equilibrium is established in which there are fewer active sites and steady-state rate is achieved.

The fact that methane formation rate is approximately first order in hydrogen partial pressure may appear to be contradictory to a reduction in the number of active sites upon an increase in hydrogen partial pressure; however, the mode by which methane is formed makes a higher steady state rate with fewer active sites possible. Both CO + CO<sub>2</sub> and methane formation rates decrease simultaneously over 1% conversion upon exposure of chars to hydrogen, indicating that sites active for both must be affected. Unlike oxygen exchange, methane formation must be preceded by hydrogen adsorption, so an unsaturated carbon site is not always needed to form methane. Oxidation does require an unsaturated site, of which there are fewer under higher hydrogen partial pressure.

Our findings lead us to conclude that annealed Saran char is covered with two types of active sites. The most abundant are those that acquire dissociatively adsorbed hydrogen from the gas phase to cover much of the char surface, achieving a bulk H/C ratio as high as 0.1 at about 70% conversion. The second type of sites are active for gasification, with competition between oxidation and methane formation reactions. Under low hydrogen partial pressure the driving force for reverse oxygen exchange is small, as is the driving force for methane formation. Thus, C(O) formation at active sites dominates and CO is the primary product, with CO<sub>2</sub> subsequently formed via the shift reaction. As hydrogen partial pressure is increased the case is reversed. The reverse oxygen exchange driving force is increased as is methane formation. The total number of unsaturated surface carbons is reduced over 1% conversion by adsorbing hydrogen until an equilibrium is reached with active site competition. Methane formation includes hydrogen adsorption onto the char surface, while oxygen exchange requires unsaturated active sites. The oxygen exchange reaction will always have to compete with the methane formation reaction for unsaturated active sites, while the methane formation reaction does not have to compete with the oxygen exchange reaction since methane formation can occur at sites that have been saturated with hydrogen.

## CONCLUSIONS

Reverse oxygen exchange and dissociative hydrogen adsorption both inhibit steam gasification of annealed Saran char, which is covered with two major types of active sites. The first and most abundant type of site dissociatively adsorbs hydrogen throughout the course of reaction, and is inactive for gasification. The second type of site is active in gasification to form CO and methane, but can become blocked with dissociatively adsorbed hydrogen upon exposure to increased hydrogen partial pressure. Reverse oxygen exchange, however, always influences CO formation. The total concentration of sites which are active towards gasification, as well as the equilibrium at these sites between oxidation, methane formation, and site blockage determines char gasification rate.

## ACKNOWLEDGMENT

The support of the United States Department of Energy (UCR Program) through Grant # DE-FG22-93PC93213 is gratefully acknowledged.

## REFERENCES

1. Montet, G.L. and Myers, G.E., Carbon **9**, 673 (1971).
2. Toomajian, M.E., Lussier, M.G., and Miller, D.J., Fuel **71**, 1055 (1992).
3. Huttinger, K.J. and Merdes, W.F., Carbon **30**(6), 883 (1992).
4. Redmond, J.P. and Walker, P.L.Jr., J. Phys. Chem. **64**, 1093 (1960).
5. Gadsby, J., Hinshelwood, C.N., and Sykes, K.W., Proc. Royal Soc. London **A187**, 129 (1946).
6. Giberson, R.C. and Walker, J.P., Carbon **3**, 521 (1966).
7. Yang, R.T. and Duan, R.Z., Carbon **23**(3), 325 (1985).
8. Blackwood, D.J. and McGrory, F., Aust. J. Chem. **11**, 16 (1958).
9. Mims, C.A. and Pabst, J.K., ACS Div. Fuel Chem. Prepr. **25**(3), 263 (1980).
10. Huttinger, K.J., Carbon **26**(1), 79 (1988).

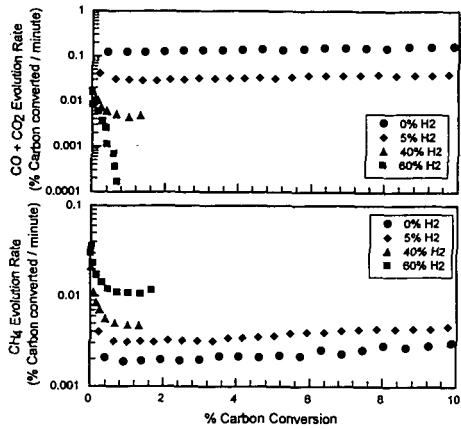


Figure 1: H<sub>2</sub>O/H<sub>2</sub> Gasification Rate of Annealed Saran Char at 1.0 MPa

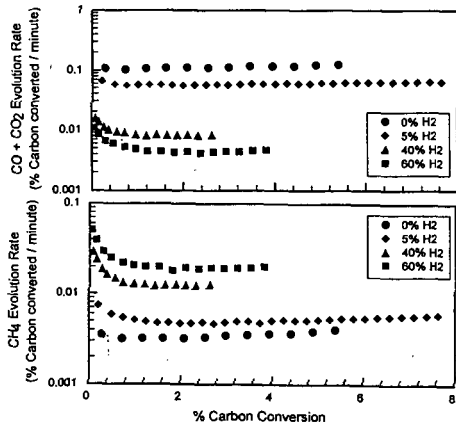


Figure 2: H<sub>2</sub>O/H<sub>2</sub> Gasification Rate of Annealed Saran Char at 3.1 MPa

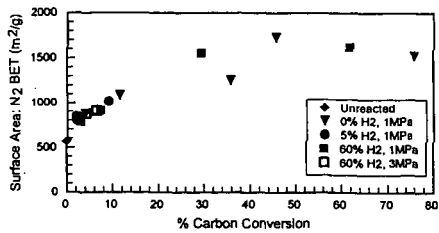


Figure 3: Surface Area (N<sub>2</sub> BET) of Annealed Saran Char Following H<sub>2</sub>O/H<sub>2</sub> Gasification

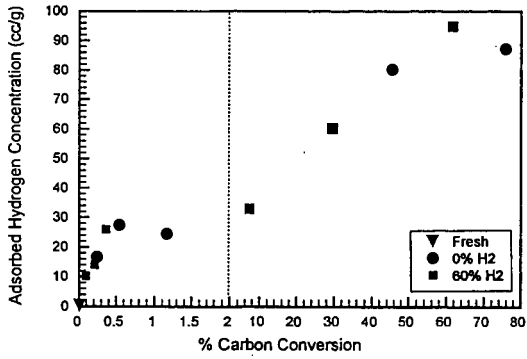


Figure 4: Adsorbed Hydrogen Concentration per Unit Weight on Annealed Saran Char Following H<sub>2</sub>O/H<sub>2</sub> Gasification at 1.0 MPa

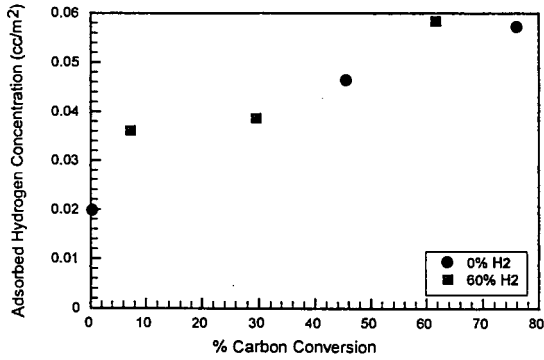


Figure 5: Adsorbed Hydrogen Concentration per Unit Surface Area on Annealed Saran Char Following H<sub>2</sub>O/H<sub>2</sub> Gasification at 1.0 MPa

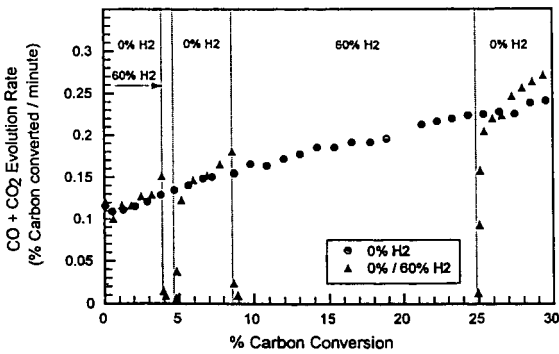


Figure 6: H<sub>2</sub>O/H<sub>2</sub> Gasification Rate of Annealed Saran Char at 1.0 MPa, Step Changes in Reactant Gas Composition